Author Manuscript

Author Manuscript

Author Manuscript

Author Manuscript

HHS Public Access

Author manuscript

J Vis Exp. Author manuscript; available in PMC 2021 July 16.

Vascular Casting of Adult and Early Postnatal Mouse Lungs for Micro-CT Imaging

Russell H. Knutsen[1], **Leah M. Gober**[1], **Joseph R. Sukinik**[1], **Danielle R. Donahue**[2], **Elise K. Kronquist**[1], **Mark D. Levin**[1], **Sean E. McLean**[3], **Beth A. Kozel**[1]

[1]Translational Vascular Medicine Branch, National Heart Lung and Blood Institute, National Institutes of Health

[2]Mouse Imaging Facility, National Institute of Neurological Disorders and Stroke, National Institutes of Health

[3]Division of Pediatric Surgery, Department of Surgery, University of North Carolina at Chapel Hill

Abstract

Blood vessels form intricate networks in 3-dimensional space. Consequently, it is difficult to visually appreciate how vascular networks interact and behave by observing the surface of a tissue. This method provides a means to visualize the complex 3-dimensional vascular architecture of the lung.

To accomplish this, a catheter is inserted into the pulmonary artery and the vasculature is simultaneously flushed of blood and chemically dilated to limit resistance. Lungs are then inflated through the trachea at a standard pressure and the polymer compound is infused into the vascular bed at a standard flow rate. Once the entire arterial network is filled and allowed to cure, the lung vasculature may be visualized directly or imaged on a micro-CT (μCT) scanner.

When performed successfully, one can appreciate the pulmonary arterial network in mice ranging from early postnatal ages to adults. Additionally, while demonstrated in the pulmonary arterial bed, this method can be applied to any vascular bed with optimized catheter placement and endpoints.

Introduction

The focus of this technique is the visualization of pulmonary arterial architecture using a polymer-based compound in mice. While extensive work has been performed on systemic vascular beds such as brain, heart, and kidney[1,2,3,4,5], less information is available regarding the preparation and filling of the pulmonary arterial network. The aim of this study, therefore, is to expand upon previous work[6,7,8] and provide a detailed written and visual reference that investigators can easily follow to produce high-resolution images of the pulmonary arterial tree.

Corresponding Author: **Beth A. Kozel**, Beth.kozel@nih.gov.

Disclosures

The authors have nothing to disclose

Author Manuscript Author Manuscript Author Manuscript Author Manuscript

While numerous methods exist for labeling and imaging lung vasculature, such as magnetic resonance imaging, echocardiography, or CT angiography[9,10], many of these modalities fail to adequately fill and/or capture the small vessels, limiting the scope of what can be studied. Methods such as serial sectioning and reconstruction provide high resolution but are time/labor-intensive[11,12,13]. Surrounding soft tissue integrity is compromised in traditional corrosion casting[10,13,14,15,16]. Even animal age and size become factors when attempting to introduce a catheter or, the resolution is lacking. The polymer injection technique, on the other hand, fills arteries to the capillary level and when combined with μCT, allows for unparalleled resolution[5]. Samples from mouse lungs as young as postnatal day 14 have been successfully casted[8] and processed in a matter of hours. These can be rescanned indefinitely, or even sent for histological preparation/electron microscopy (EM) without compromising the existing soft tissue[17]. The main limitations to this method are the upfront cost of CT equipment/software, challenges with accurately monitoring intravascular pressure, and the inability to acquire data longitudinally in the same animal.

This paper builds on existing work to further optimize the pulmonary artery injection technique and push age/size related boundaries down to postnatal day 1 (P1) to yield striking results. It is most useful for teams that want to study arterial vascular networks. Accordingly, we provide new guidance for catheter placement/stabilization, increased control over fill rate/volume, and highlight notable pitfalls for increased casting success. Resulting casts can then be used for future characterization and morphologic analysis. Perhaps more importantly, this is the first visual demonstration, to our knowledge, that walks the user through this intricate procedure.

Protocol

All methods described here have been approved by the Institutional Animal Care and Use Committee (ACUC) of the National Heart Lung and Blood Institute.

1. Preparation

1. Inject the mouse intraperitoneally with heparin (1 unit/g mouse body weight) and allow it to ambulate for 2 min.
2. Euthanize the animal in a CO_2 chamber.
3. Arrange the mouse in a supine position on a surgical board and secure all four limbs to the board with tape. Use magnification for fine dissection.

2. Exposing lungs and trachea

1. Spray the ventral side of the mouse with 70% ethanol to minimize hair interference.
2. Grasp the abdominal skin with forceps and make a small incision with scissors in the umbilical region. Slide the tips of scissors into the fascial layer between the abdominal musculature and skin and begin separating the two layers. Work rostrally, removing the skin from the abdomen, ribcage, and neck.

Author Manuscript Author Manuscript Author Manuscript Author Manuscript

3. Open the abdominal musculature with scissors and cut laterally on both sides until the diaphragm is exposed.

4. Gently grasp the xiphoid process and slightly lift the ribcage maximizing the view of the caudal lungs through the thin, semitransparent diaphragm. Carefully make a small incision in the diaphragm just beneath the xiphoid process. The lungs will collapse and retract away from the diaphragm. Dissect the diaphragm away from the ribcage, taking care not to nick the lung parenchyma.

5. Locate and sever the inferior vena cava (IVC) and esophagus where they pass through the diaphragm. Use gauze to clean up any pooling blood in the thoracic cavity, avoiding contact with the lungs.

6. Grasp the xiphoid once again and gently lift. Cut the ribcage bilaterally (roughly at the midaxillary line) avoiding contact with the lungs. Remove the anterior ribcage entirely, making the final cut along the sternal angle just before the manubrium.

7. Using a prefilled syringe, liberally wet the lungs with phosphate-buffered saline (PBS, pH 7.4) to prevent drying out. Continue this routine throughout the procedure.

8. Using forceps, grasp the manubrium and gently elevate away from the body. Using scissors, cut 1-2 mm lateral to the manubrium, severing clavicles, and remove. This will expose the thymus underneath.

9. Grasp each lobe of the thymus, pull apart, and remove. Repeat this procedure with the submandibular gland. Finally, remove the muscular tissue overlaying the trachea.

   NOTE: Following the dissection, the heart, ascending aorta (AA), pulmonary arterial trunk (PAT), and trachea should be visible. Ensure the primary arterial branches off the trunk are not divided or injured.

3. PA catheterization and blood perfusion

1. To assemble Unit 1, thread 15 cm of PE-10 tubing onto the hub of a 30 G needle and attach to a 1 mL syringe prefilled with 10^{-4} M sodium nitroprusside (SNP) in PBS. Prime the tubing by advancing the plunger until all the air is purged from this unit (Figure 1).

   CAUTION: SNP is toxic if swallowed. Avoid contact with the skin and eyes. Wash skin thoroughly after handling. Wear appropriate personal protective equipment.

   1. Alternatively, assemble Unit 2. For mice postnatal day 7 (P7) and younger, use a hemostat to detach an additional 30 G needle from its hub and thread the needle onto the open end of the tubing of Unit 1 (Figure 1).

2. Instead of a needle, use curved sharp forceps to grasp one end of a 10 cm length of 7-0 silk. Penetrate the apex of the heart entering from one side and passing the

Author Manuscript Author Manuscript Author Manuscript Author Manuscript

tips of the forceps through the muscle and out of the other side. Grasp the silk with another set of forceps and pull approximately a 2 cm length through and tie off. Take the remaining 8 cm end of the suture, tugging the heart caudally, and tape the end to the surgical board.

NOTE: This will create tension, further exposing the great vessels and tethering the heart in place, allowing for easier placement of the catheter in the pulmonary artery.

3. Hook the tips of curved forceps under both the AA and PAT. Pull a 3 cm length of 7-0 silk back through the opening and create a single-throw loose suture.

4. Using scissors make a 1-2 mm incision toward the apex of the heart, penetrating the thin-walled right ventricle (RV), to allow for the insertion of the catheter (Unit 1). Prior to the insertion, confirm there is no air in the system. Introduce the primed tubing into the right ventricle and gently advance into the semitransparent thin-walled PAT.

    1. Visually verify that the catheter has not advanced into either the left or right pulmonary branches and does not abut the pulmonary artery branchpoint. Using tape, secure the distal portion of the tubing to the surgical board.

        NOTE: To identify the RV, use forceps to pinch the right side of the heart. Unlike the left ventricle, the relatively thin free wall of the RV should be easily grasped.

    2. For mice younger than P7, attach Unit 2 to a micromanipulator and introduce the needle end of the unit into the PAT as described above using the manipulator.

5. Gently tighten the loose suture around both great vessels and cut the 8 cm length of suture created in step 3.2 to return the heart to a natural resting position. The catheter is now firmly secured within the PAT.

6. Clip the left auricle of the heart to allow perfusate to exit the system.

7. Secure SNP-containing syringe (Unit 1 or Unit 2, size dependent) in the syringe pump and perfuse the solution at a rate of 0.05 mL/min to flush the blood and maximally dilate the vasculature. Blood/perfusate will exit via the clipped auricle. Continue perfusion until perfusate runs clear (~200 μL in an adult mouse, less for younger animals).

    NOTE: When perfusing the low viscosity PBS/SNP, a relatively higher infusion rate was used in the interest of saving time. The more viscous polymer compound is infused at a slower rate to prevent overfilling, rupture, and maximize control over distal endpoints.

4. Tracheostomy and lung inflation

1. Construct the lung inflation unit (Figure 2).

Author Manuscript Author Manuscript Author Manuscript Author Manuscript

1. Connect a flexible plastic 24 G intravenous (IV) catheter (needle removed)/butterfly infusion set to a stopcock, attached to an open 50 mL syringe (no plunger). Hang the syringe from a ring stand.

2. Add 10% buffered formalin to the syringe. Open the stopcock, allowing formalin to enter the tubing and purge all air from the system. Close the stopcock and raise the syringe until the meniscus is 20 cm above the trachea[8].

   CAUTION: Formalin is flammable, carcinogenic, acutely toxic when ingested, and causes skin irritation, serious eye damage, skin sensitization, and germ cell mutagenicity. Avoid ingestion and contact with skin and eyes. Avoid inhalation of the vapor or mist. Keep away from sources of ignition. Wear appropriate personal protective equipment.

2. Place two loose sutures inferior to the cricoid cartilage 2-4 mm apart.

3. Using scissors, make a small incision in the cricothyroid ligament superior to the sutures.

4. Insert the IV catheter into the opening and advance the tip beyond the two loose sutures.

5. Tighten the sutures around the trachea and open the stopcock. Allow the formalin to enter the lungs by gravity and wait for 5 min for the lungs to fully inflate. If the lungs adhere to the ribcage during inflation, grasp the outside of the ribcage with blunt tipped forceps and move in all directions to assist in freeing the lobes. Do not make direct contact with lungs.

6. After 5 min, back the IV catheter beyond the first suture and ligate. Repeat for the second suture. The lungs are now inflated in a closed, pressurized state.

5. Casting the vasculature

1. In a 1.5 mL tube, prepare 1 mL of an 8:1:1 solution[8] of polymer:diluent:curing agent and gently invert several times to ensure good mixing.

2. Remove the plunger from a 1 cc syringe, cover the opposite end with a gloved finger, and pour the polymer compound into the syringe. Carefully reinsert the plunger, invert, and advance the plunger to remove all air and form a meniscus at the tip of the syringe.

3. Remove the SNP/PBS syringe from the hub of the needle and drip additional PBS into the hub to create a meniscus. Carefully check the hub for trapped air, dislodge if necessary, and reform the meniscus. Join the hub to the syringe filled with the polymer compound.

   NOTE: Creating a meniscus on both ends significantly reduces the chance for air to enter the system.

Author Manuscript Author Manuscript Author Manuscript Author Manuscript

4. Attach the polymer compound filled syringe to the syringe pump and infuse at 0.02 mL/min.

   NOTE: For smaller lungs, a slower rate can be helpful to prevent overfilling but, is not essential.

5. Monitor the compound as it freely moves down the PE tubing and note the syringe volume as it enters the PAT. Continue filling until all lobes are filled completely down to the capillary level and stop the syringe pump. Check the syringe volume again.

   NOTE: After several runs an estimated volume can be used to gauge an approximate endpoint (~35 μL for an adult mouse and ~5 μL for a P1 pup). After the pump is halted, the residual pressure in the system will continue to push the polymer compound into the pulmonary arteries. All lung lobes should fill at a similar rate.

6. Cover the lungs with a fiber optic cleaning wipe, liberally apply PBS, and allow the carcass to sit undisturbed for 30-40 min at room temperature. During this period, the polymer compound will cure and harden.

7. Remove the catheter, sever the arms/lower half of the mouse, and place the head/thorax into a 50 mL conical filled with 10% buffered formalin overnight.

8. After fixation, grasp the trachea and gently separate the heart/lung unit from the remaining rib cage and thorax. Place the heart/lung block in a formalin filled scintillation vial. Discard the rest.

6. Alternative vascular beds for casting (Table 1)

NOTE: Each target vascular bed may require different catheter placements, infusion rates, and optimal filling times. Thus, multiple animals will be necessary to cast multiple organs.

1. For systemic vascular beds superior or inferior to the diaphragm follow steps 1.1-2.5 as above. See additional notes on the portal system and diaphragm (Table 1).

2. Grasp the xiphoid process with a hemostat and cut the ribcage bilaterally (roughly in the midaxillary line) just prior to the internal thoracic arteries.

3. Fold the still connected ribcage over such that it is resting on the animal's neck/head, fully exposing the chest cavity.

4. Follow step 3.1 above, then remove the lungs. Once the thoracic aorta (TA) is visible, hook the tips of curved forceps underneath it, ~10 mm superior to the diaphragm. Grasp a 3 cm length of 7-0 silk, pull back through the opening under the TA, and create a single-throw loose suture. Repeat this procedure ~8 mm above the diaphragm.

5. For structures superior to the diaphragm, use spring scissors to create a small hole (~30% of the total circumference) on the ventral portion of the TA, ~2 mm inferior to the loose sutures placed in step 6.4.

Author Manuscript Author Manuscript Author Manuscript Author Manuscript

1. For structures inferior to the diaphragm, instead, create a small hole ~2 mm superior to the loose sutures.

6. Depending on the animal size, introduce Unit 1 or 2 into the vessel, advance beyond loose sutures, and gently ligate the vessel.

7. Follow step 3.7, setting the syringe pump at a rate of 1.0 mL/min and perfusing a minimum of 5 mL. Perfusate will exit via the IVC.

8. Follow steps 5.1 - 5.4 adjusting the infusion rate to 0.05 mL/min, visually monitoring the target tissue in real-time.

   NOTE: Infusion volume will be organ and animal age specific. The volume can be further limited by ligating arterial branches leading to non-target vascular beds (i.e., brain, liver, kidney, intestine).

9. Follow 5.6 then remove target tissue and place in formalin.

7. Sample mount, scan, and reconstruction for micro-CT

1. Using paraffin film, create a flat surface on the scanning bed and center the wet sample on this surface (Figure 3A).

   NOTE: If motion artifact is detected, the sample may require further stabilization.

2. Lightly tent/cover sample with additional paraffin film to prevent dehydration. Take special care not to rest the paraffin film on the sample causing deformation to the tissue (Figure 3B).

3. Scan the sample using settings outlined in Table 2 and standardize these parameters within a given experiment.

   NOTE: This is experiment/endpoint dependent. Standardize the chosen parameters for the ease of comparison between samples.

4. Transfer the reconstructed scans for post-processing and analysis.

Representative Results

A successful cast will exhibit uniform filling of the entire pulmonary arterial network. We demonstrate this in C57BI/6J mice ranging in age: Postnatal day P90 (Figure 4A), P30 (Figure 4B), P7 (Figure 4C), and P1 (Figure 4D). By controlling the rate of flow and visually monitoring the fill in real-time, reliable endpoints of the most distal vasculature were achieved (Figure 5A).

Common challenges include damage to the lungs, incomplete filling, underfilling, or overfilling, wedging the catheter, and animal size.

If there is damage to the lung/airway, small leaks will prevent the lungs from holding pressure (Figure 5B,C). In the absence of complete inflation, it becomes difficult to make accurate quantitative and spatial comparisons across samples. To minimize the risk to the

Author Manuscript Author Manuscript Author Manuscript Author Manuscript

lung parenchyma, avoid cutting too closely to the lungs when removing the ribcage and keep the lungs moist with PBS throughout the procedure to avoid dehydration and adherence to surrounding structures. If a lobe adheres to the rib cage during inflation, gently grasp the outside of the ribcage (away from the lung) with forceps and move it in a direction to free the lobes. Alternatively, a blunt instrument, such as a spatula, with a smooth edge can be used to lift or push the inflated lung away from the ribcage. When inflating the lungs, adhere to suggested pressure parameters and avoid over-inflation as this can lead to rupture of the airway. Finally, do not remove lungs from thoracic cavity until post-fixation is complete. The trachea, lungs, and heart should be removed en bloc from the remaining portions of the thoracic cavity.

Patchy (Figure 5D) or incomplete (Figure 5E) filling can arise from an “airlock”, in which air is introduced into the vascular system via the catheter, blocking downstream flow of the compound. To minimize the chance of an airlock, vigilantly purge air from the tip of the catheter prior to insertion (Step 3.4) and during the syringe transition from SNP/PBS to polymer compound. If the fill remains patchy or incomplete, it could be an indication of increased vascular resistance as a result of focal/long segment stenosis or tortuosity. Blood clots can also lead to incomplete filling and are easily avoided by using heparin prior to the procedure.

Improper injection volume will lead to underfilling or overfilling. Underfilling occurs when too little compound is introduced into the vasculature (Figure 5F). Alternatively, overfilling, or introducing too much polymer compound too rapidly can cause either arterial rupture (Figure 5G) or, more commonly, venous transit (Figure 5H). Both problems can be alleviated by using a syringe pump. Investigators should carefully adhere to the proposed rate and volume restrictions or establish their own rates based upon their specific model and optimization. Monitoring polymer compound perfusion in real time under magnification is critical, and filling of small arterioles/capillaries should be used as an endpoint.

Advancing the catheter too far down the pulmonary trunk can cause the tip to wedge into one pulmonary artery branch and create an imbalance in the flow. As a result, one side fills faster than the other (Figure 5I), which frequently leads to overfilling in one lung and underfilling in the other. While catheter wedging is the most likely reason in this scenario, “airlock” and lack of heparin can also be contributing factors.

Finally, smaller animals present their own set of additional obstacles. Younger animals demand steady hands and small mistakes are less forgiving. High quality instruments, specifically designed for microsurgery, become more important at early postnatal timepoints. Use of a micromanipulator assists greatly in not only placement but preventing catheter dislocation. It is also essential to utilize the syringe pump on small animals to accurately control and manage endpoints.

While specifically shown for the pulmonary vasculature, this procedure can easily be applied to systemic target vascular beds as well (Table 1). In addition to the challenges listed above, choosing the right entry point is crucial. Casting via the thoracic aorta produces excellent results for most vascular beds. It should be noted, however, that inserting the catheter as

Author Manuscript Author Manuscript Author Manuscript Author Manuscript

proximal to the target site as possible and ligating non-target vasculature assists in flow and volume control. These refinements combined with appropriate direct monitoring of distal vascular endpoints (Figure 6A–F) and standard infusion rates optimize the filling. Many examples of such casting methods exist in the literature and are too numerous for complete referencing. However, additional details may be found in organ specific text such as these[4,5,7,18,19,20,21].

After casting, samples can be processed for μCT scanning (Figure 7A,B). For post-processing, a commercial software package (see Table of Materials) produced a 3D volume rendering of the pulmonary vascular tree presented as still images (Figure 7C), or movies. Further statistical analyses exploring vascular characteristics such as segment length and number, tortuosity, order (generation or rank), volume, and arcade length can also be performed. In addition to μCT scanning, the casted samples can also be cleared to obtain gross images or processed and cut for histological analysis[8].

Discussion

Executed properly, this method yields striking images of pulmonary arterial networks, allowing for comparison and experimentation in rodent models. Several critical steps along the way ensure success. First, investigators must heparinize the animal in the preparatory stage to prevent blood clots from forming in the pulmonary vasculature and chambers of the heart. This allows for the complete arterial transit of polymer compound. Second, when puncturing the diaphragm and removing the ribcage, take care to protect the lungs from inadvertent damage, cuts or injury. Any leak in the airway will prevent complete inflation and render comparisons between samples inaccurate. Third, tethering the heart at the apex aids catheter placement. Fourth, the use of a strong vasodilator such as SNP will assist in both the removal of blood and complete filling of arterioles and capillaries[5,8]. Fifth, when placing the catheter into the PAT, take care not to bury the tip into the bifurcation. This will cause an imbalance in flow, shunting polymer compound to either the left or right side, yielding an unequal pressure gradient. Sixth, the use of a syringe pump will allow the user to control the rate and titer the volume to both mouse strain and age. Lastly, leave the heart/lungs attached to the remainder of the thoracic cavity, fix overnight, and remove the following day. The lungs will be well fixed and the potential for deflation due to accidental nicks during separation will be minimized.

While this methodology achieves the desired results, alternative techniques may be helpful to some users. To aid in the placement of the catheter, a micromanipulator may be employed. We chose a version with a small profile and magnetic base to minimize encroachment in an already limited working area while providing a stable base (if using a magnetic base make sure to place a steel plate under the working space to allow the magnet to engage). This allows the user to precisely place the tip of the catheter in the PAT at an angle that follows the natural trajectory of the artery. Additionally, the catheter is secure and at less risk of being dislodged. Another option is the use of a trumpeted catheter tip[8]. While not trivial to create, a trumpeted catheter is far more secure and less inclined to accidentally slide out of the PAT. Changing the ratio of polymer:diluent alters the viscosity and the ease with which small vessels are filled. Depending on the target vasculature and experimental endpoints this

Author Manuscript Author Manuscript Author Manuscript Author Manuscript

can be a valuable consideration. Euthanasia via CO_2 may cause pulmonary hemorrhage in a small percentage of animals and is strain dependent[22]. Consider an alternative euthanasia protocol should this impact experimental endpoints. When inflating the lungs, the use of formalin aids fixation of the organ in place at the given pressure. A physiologically neutral buffer can be substituted should peripheral vessels need to be filled in an unfixed state. If infusion rate and control are of less importance to a given experiment, perfusion by hand is also possible. Hand injection requires practice and real-time monitoring under magnification to avoid overfilling or vessel rupture[8]. Finally, the tissue mount/conditions, scanning parameters, and minimal post-processing we employed for this paper should serve merely as a starting point. Different scanners, tissues, experimental endpoints/user needs may demand alternative parameters.

While the vascular images generated from this technique are impressive, there are limitations. Primarily, the above method is suboptimal for measuring vascular caliber due to the inability to monitor and control intravascular pressure during the infusion. Other groups have managed to somewhat address these pressure concerns in systemic vasculature by monitoring driving pressure[4,23], however, such concerns are further amplified on the pulmonary side due to the relatively thin pulmonary artery walls that are easily distensible with small changes in pressures[24] and the inability to precisely measure and statically control pulmonary intravascular pressure.

A second limitation to this method is that it remains a postmortem, single timepoint experiment, limiting its utility in studies that require truly physiologic conditions or a time course. Other, live animal measures, such as CT pulmonary angiography (CTPA) or contrast-enhanced μCT (CE-CT) offer the possibility of functional and morphologic measures. Repeated scans/longitudinal studies as well as measurements at different points in the cardiac/pulmonary cycle, can be explored[10,25,26,27,28]. These methods can be reliably used, in addition to echocardiography, to measure the arterial caliber. However, both CTPA and echocardiography measures are currently limited to the assessment of the proximal vasculature. For echocardiogram, the assessment is limited to the pulmonary trunk while CTPA allows adequate calculation of the branch pulmonary artery caliber potentially 1-2 orders further, but resolution is limited, obscuring distal portions of the vasculature[7]. Radiation dosage is also a concern that should be carefully monitored when using CT especially in multi-scan longitudinal studies[29,30]. For either of these applications, μCT equipment, scan time, and analysis software may be expensive and require specialized staff training. Animal imaging core facilities at some institutions may ease this burden.

As an alternative to this compound, some groups utilize traditional corrosion casting techniques accompanied by soft tissue removal[31,32]. These methods yield results similar to this polymer compound, but the end product is brittle, leading to potential artifact[15]. In addition, the removal of soft tissue eliminates the potential for future histology[33]. Another option is to leave the soft tissue intact and perform a follow-up step wherein the soft tissue is “cleared” rendering the sample virtually transparent[34,35]. Tissue clearing gives the user some ability to see deeper within a sample but, on the whole, remains inferior to μCT as it cannot provide the same 3D visualization. Serial histologic sectioning and array tomography are methods that offer exceptionally high resolution. While this technique opens the door to

Author Manuscript Author Manuscript Author Manuscript Author Manuscript

exciting new possibilities, the workload is exponentially higher and not particularly conducive to large cohorts[11,12]. 3D x-ray histology is a non-destructive approach that couples both μCT and traditional histology or even EM[36,37,38].It takes a more high level view of pathology by utilizing μCT to globally identify and accurately scout regions of interest that are then followed up with routine histology[39]. Substituting lower resolution contrast agents (or in some cases no contrast) with polymer compound into the vasculature might serve to elevate both techniques when possible. Another non-destructive approach that is computationally intensive yet, potentially enhances the contrast, is phase-retrieval μCT imaging[40,41]. This method can be valuable when employed on noisy data where contrast is weak or not possible[42].The polymer compound employed in this technique, however, does not suffer from this limitation. That said, phase-retrieval may be useful where the polymer compound is possibly diluted, for example in distal vasculature[43]. Finally, stereology has been a standard in lung quantitative structural analysis for years[44]. It uses random, systematic sampling on cross sections of tissue to make 3-D inferences assuming that the chosen samples are sufficiently representative. While a powerful tool, it has the potential to lead to error and bias. Combining CT imaging with stereology, however, holds great promise[45].

The outlined method is relatively straightforward and with training a success rate of >90% is achievable. Once mastered, it allows for the complete and reliable casting of lung vasculature. In fixative, tissue and polymer remain stable indefinitely for future scans, potential histology, or EM[46,47]. We've shown that this technique can be used in animals as young as P1 through adulthood and believe embryonic casting, via the pulmonary artery, is within reach. It should be noted that this technique can be applied to virtually any other vascular bed by simply altering the catheter entry point and determining appropriate endpoints.

Supplementary Material

Refer to Web version on PubMed Central for supplementary material.

Acknowledgments

This research was supported in part by the NHLBI Intramural Research Program (DIR HL-006247). We would like to thank the NIH Mouse Imaging Facility for guidance in image acquisition and analysis.

References

1. Vasquez SX, et al. Optimization of microCT imaging and blood vessel diameter quantitation of preclinical specimen vasculature with radiopaque polymer injection medium. PLoS One. 6 (4), e19099 (2011). [PubMed: 21533123]
2. Hong SH, et al. Development of barium-based low viscosity contrast agents for micro CT vascular casting: Application to 3D visualization of the adult mouse cerebrovasculature. Journal of Neuroscience Research. 98 (2), 312–324 (2019). [PubMed: 31630455]
3. Perrien DS, et al. Novel methods for microCT-based analyses of vasculature in the renal cortex reveal a loss of perfusable arterioles and glomeruli in eNOS−/− mice. BMC Nephrology. 17, 24 (2016). [PubMed: 26936597]

Author Manuscript Author Manuscript Author Manuscript Author Manuscript

4. Weyers JJ, Carlson DD, Murry CE, Schwartz SM,Mahoney WM Jr., Retrograde perfusion and filling of mouse coronary vasculature as preparation for micro computed tomography imaging. Journal of Visualized Experiments. (60), e3740, (2012). [PubMed: 22353785]
5. Zhang H, Faber JE, De-novo collateral formation following acute myocardial infarction: Dependence on CCR2(+) bone marrow cells. Journal of Molecular and Cellular Cardiology. 87, 4–16 (2015). [PubMed: 26254180]
6. Kim BG, et al. CXCL12-CXCR4 signalling plays an essential role in proper patterning of aortic arch and pulmonary arteries. Cardiovascular Research. 113 (13), 1677–1687 (2017). [PubMed: 29016745]
7. Counter WB, Wang IQ, Farncombe TH, Labiris NR, Airway and pulmonary vascular measurements using contrast-enhanced micro-CT in rodents. American Journal of Physiology Lung Cellular and Molecular Physiology. 304 (12), L831–843 (2013). [PubMed: 23564512]
8. Phillips MR, et al. A method for evaluating the murine pulmonary vasculature using micro-computed tomography. Journal of Surgical Research. 207, 115–122 (2017).
9. Schuster DP, Kovacs A, Garbow J, Piwnica-Worms D, Recent advances in imaging the lungs of intact small animals. American Journal of Respiratory Cell and Molecular Biology. 30 (2), 129–138 (2004). [PubMed: 14729505]
10. Samarage CR, et al. Technical Note: Contrast free angiography of the pulmonary vasculature in live mice using a laboratory x-ray source. Medical Physics. 43 (11), 6017 (2016). [PubMed: 27806595]
11. Grothausmann R, Knudsen L, Ochs M, Muhlfeld C, Digital 3D reconstructions using histological serial sections of lung tissue including the alveolar capillary network. American Journal of Physiology Lung Cellular and Molecular Physiology. 312 (2), L243–l257 (2017). [PubMed: 27913424]
12. Hayworth KJ, et al. Imaging ATUM ultrathin section libraries with WaferMapper: a multi-scale approach to EM reconstruction of neural circuits. Front Neural Circuits. 8, 68 (2014). [PubMed: 25018701]
13. Bussolati G, Marchio C, Volante M, Tissue arrays as fiducial markers for section alignment in 3-D reconstruction technology. Journal of Cellular and Molecular Medicine. 9 (2), 438–445 (2005). [PubMed: 15963262]
14. Preissner M, et al. Application of a novel in vivo imaging approach to measure pulmonary vascular responses in mice. Physiological Reports. 6 (19), e13875 (2018). [PubMed: 30284390]
15. Junaid TO, Bradley RS, Lewis RM, Aplin JD,Johnstone ED, Whole organ vascular casting and microCT examination of the human placental vascular tree reveals novel alterations associated with pregnancy disease. Scientific Reports. 7 (1), 4144 (2017). [PubMed: 28646147]
16. Bolender RP, Hyde DM, Dehoff RT, Lung morphometry: a new generation of tools and experiments for organ, tissue, cell, and molecular biology. American Journal of Physiology. 265 (6 Pt 1), L521–548 (1993).
17. Savai R, et al. Evaluation of angiogenesis using micro-computed tomography in a xenograft mouse model of lung cancer. Neoplasia. 11 (1), 48–56 (2009). [PubMed: 19107231]
18. Ehling J, et al. Micro-CT imaging of tumor angiogenesis: quantitative measures describing micromorphology and vascularization. American Journal of Pathology. 184 (2), 431–441 (2014).
19. Sueyoshi R, Ralls MW, Teitelbaum DH, Glucagon-like peptide 2 increases efficacy of distraction enterogenesis. Journal of Surgical Research. 184 (1), 365–373 (2013).
20. Zhang H, Jin B, Faber JE, Mouse models of Alzheimer's disease cause rarefaction of pial collaterals and increased severity of ischemic stroke. Angiogenesis. 22 (2), 263–279 (2019). [PubMed: 30519973]
21. Faight EM, et al. MicroCT analysis of vascular morphometry: a comparison of right lung lobes in the SUGEN/hypoxic rat model of pulmonary arterial hypertension. Pulmonary Circulation. 7 (2), 522–530 (2017). [PubMed: 28597764]
22. Fisher S, Burgess WL, Hines KD, Mason GL, Owiny JR, Interstrain Differences in CO2-Induced Pulmonary Hemorrhage in Mice. Journal of the American Association for Laboratory Animal Science. 55 (6), 811–815 (2016). [PubMed: 27931322]

Author Manuscript Author Manuscript Author Manuscript Author Manuscript

23. Munce NR, et al. Intravascular and extravascular microvessel formation in chronic total occlusions a micro-CT imaging study. JACC Cardiovascular Imaging. 3 (8), 797–805 (2010). [PubMed: 20705258]
24. Shifren A, Durmowicz AG, Knutsen RH, Faury G, Mecham RP, Elastin insufficiency predisposes to elevated pulmonary circulatory pressures through changes in elastic artery structure. Journal of Applied Physiology (1985). 105 (5), 1610–1619 (2008).
25. Sonobe T, et al. Imaging of the closed-chest mouse pulmonary circulation using synchrotron radiation microangiography. Journal of Applied Physiology (1985). 111 (1), 75–80 (2011).
26. Ritman EL, Micro-computed tomography of the lungs and pulmonary-vascular system. Proceedings of the American Thoracic Society. 2 (6), 477–480 (2005). [PubMed: 16352751]
27. Dinkel J, et al. Intrinsic gating for small-animal computed tomography: a robust ECG-less paradigm for deriving cardiac phase information and functional imaging. Circulation: Cardiovascular Imaging. 1 (3), 235–243 (2008). [PubMed: 19808548]
28. Ashton JR, West JL, Badea CT, In vivo small animal micro-CT using nanoparticle contrast agents. Frontiers in Pharmacology. 6, 256 (2015). [PubMed: 26581654]
29. Ford NL, Thornton MM, Holdsworth DW, Fundamental image quality limits for microcomputed tomography in small animals. Medical Physics. 30 (11), 2869–2877 (2003). [PubMed: 14655933]
30. Boone JM, Velazquez O, Cherry SR, Small-animal X-ray dose from micro-CT. Molecular Imaging. 3 (3), 149–158 (2004). [PubMed: 15530250]
31. Giuvarasteanu I, Scanning electron microscopy of vascular corrosion casts--standard method for studying microvessels. Romanian Journal of Morphology and Embryology. 48 (3), 257–261 (2007). [PubMed: 17914492]
32. Polguj M, et al. Quality and quantity comparison study of corrosion casts of bovine testis made using two synthetic kits: Plastogen G and Batson no. 17. Folia Morphologica (Warsz). 78 (3), 487–493 (2019).
33. Verli FD, Rossi-Schneider TR, Schneider FL, Yurgel LS, de Souza MA, Vascular corrosion casting technique steps. Scanning. 29 (3), 128–132 (2007). [PubMed: 17477397]
34. Azaripour A, et al. A survey of clearing techniques for 3D imaging of tissues with special reference to connective tissue. Progress in Histochemistry and Cytochemistry. 51 (2), 9–23 (2016). [PubMed: 27142295]
35. Richardson DS, Lichtman JW, Clarifying Tissue Clearing. Cell. 162 (2), 246–257 (2015). [PubMed: 26186186]
36. Albers J, Markus MA, Alves F, Dullin C, X-ray based virtual histology allows guided sectioning of heavy ion stained murine lungs for histological analysis. Scientific Reports. 8 (1), 7712 (2018). [PubMed: 29769600]
37. Katsamenis OL, et al. X-ray Micro-Computed Tomography for Nondestructive Three-Dimensional (3D) X-ray Histology. American Journal of Pathology. 189 (8), 1608–1620 (2019).
38. Morales AG, et al. Micro-CT scouting for transmission electron microscopy of human tissue specimens. Journal of Microscopy. 263 (1), 113–117 (2016). [PubMed: 26854176]
39. Wen H, et al. Correlative Detection of Isolated Single and Multi-Cellular Calcifications in the Internal Elastic Lamina of Human Coronary Artery Samples. Scientific Reports. 8 (1), 10978 (2018). [PubMed: 30030502]
40. Zamir A, et al. Robust phase retrieval for high resolution edge illumination x-ray phase-contrast computed tomography in non-ideal environments. Scientific Reports. 6, 31197 (2016). [PubMed: 27502296]
41. Yu B, et al. Evaluation of phase retrieval approaches in magnified X-ray phase nano computerized tomography applied to bone tissue. Optics Express. 26 (9), 11110–11124 (2018). [PubMed: 29716036]
42. Bidola P, et al. Application of sensitive, high-resolution imaging at a commercial lab-based X-ray micro-CT system using propagation-based phase retrieval. Journal of Microscopy. 266 (2), 211–220 (2017). [PubMed: 28181677]
43. Norvik C, et al. Synchrotron-based phase-contrast micro-CT as a tool for understanding pulmonary vascular pathobiology and the 3-D microanatomy of alveolar capillary dysplasia. American

Author Manuscript Author Manuscript Author Manuscript Author Manuscript

Journal of Physiology Lung Cellular and Molecular Physiology. 318 (1), L65–l75 (2020). [PubMed: 31596108]

44. Weibel ER, Lung morphometry: the link between structure and function. Cell and Tissue Research. 367 (3), 413–426 (2017). [PubMed: 27981379]
45. Hsia CC, Hyde DM, Ochs M, Weibel ER, An official research policy statement of the American Thoracic Society/European Respiratory Society: standards for quantitative assessment of lung structure. American Journal of Respiratory and Critical Care Medicine. 181 (4), 394–418 (2010). [PubMed: 20130146]
46. Sarhaddi D, et al. Validation of Histologic Bone Analysis Following Microfil Vessel Perfusion. Journal of Histotechnology. 35 (4), 180–183 (2012). [PubMed: 26207077]
47. Ehling J, et al. Quantitative Micro-Computed Tomography Imaging of Vascular Dysfunction in Progressive Kidney Diseases. Journal of the American Society of Nephrology. 27 (2), 520–532 (2016). [PubMed: 26195818]

Author Manuscript Author Manuscript Author Manuscript Author Manuscript

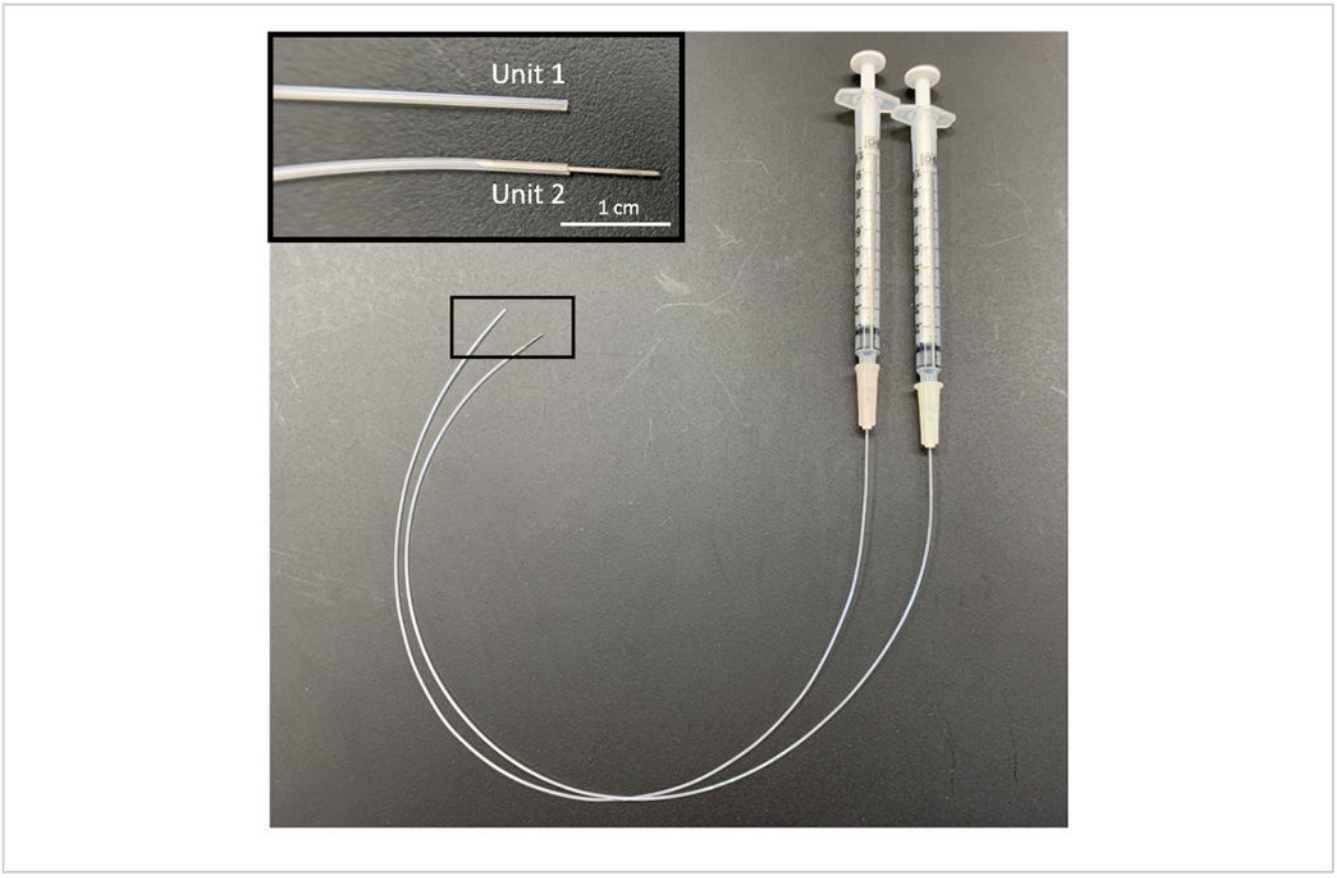

Figure 1: Catheter and needle setup.
Syringes are shown with attached tubing and needles (Unit1 and Unit2). Inset: closeup of needle and tubing.

Author Manuscript Author Manuscript Author Manuscript Author Manuscript

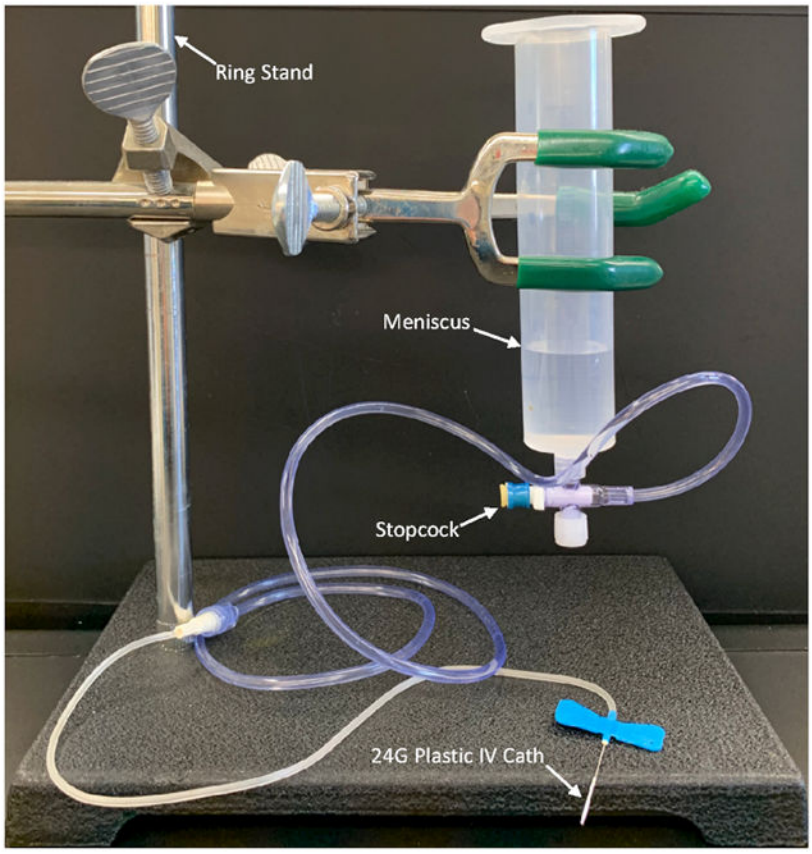

Figure 2: Lung inflation setup.
Ring stand, clamp, a syringe filled with formalin, and tubing with a catheter attached.

Author Manuscript Author Manuscript Author Manuscript Author Manuscript

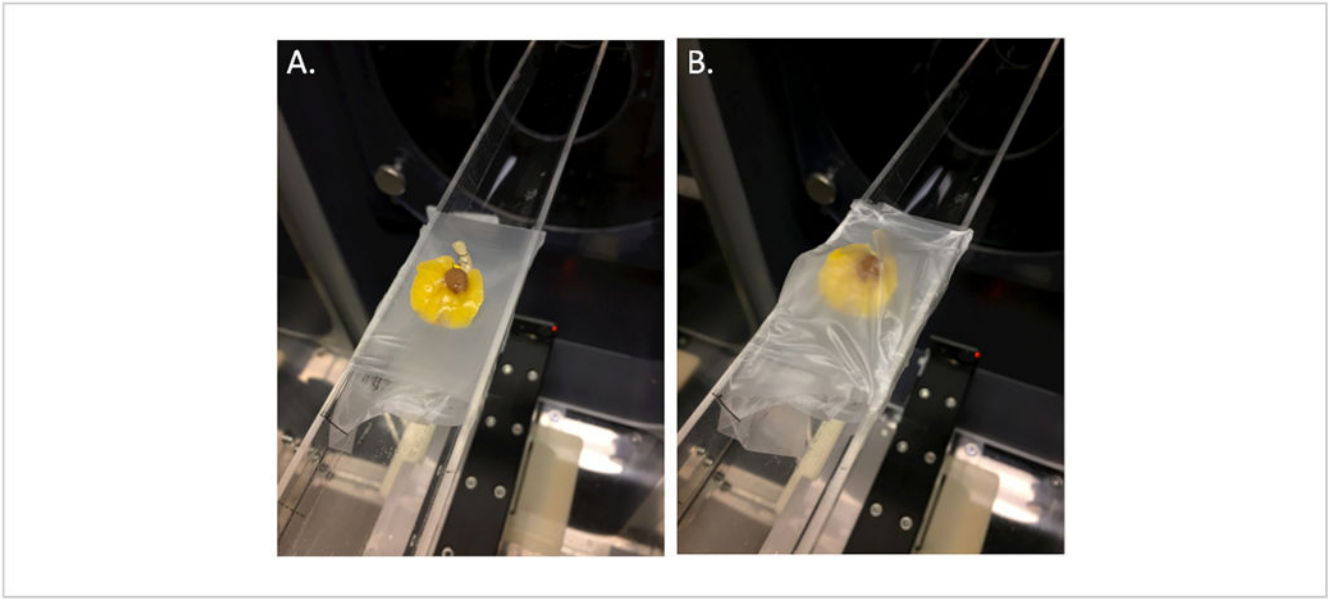

Figure 3: Micro-CT sample preparation pre-scan.
(**A**) Here the specimen was centered on a paraffin film base, (**B**) Here the sample was centered and covered on the parafilm base.

Author Manuscript Author Manuscript Author Manuscript Author Manuscript

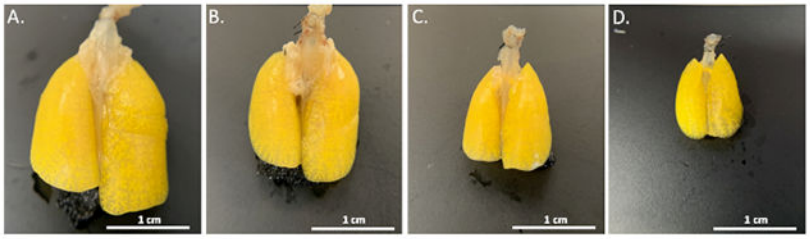

Figure 4: Vascular-casted lungs at varying developmental stages from 3 months to 1 day old.
Dorsal view of lungs, (**A**) P90, (**B**) P30, (**C**) P7, and (**D**) P1

Author Manuscript Author Manuscript Author Manuscript Author Manuscript

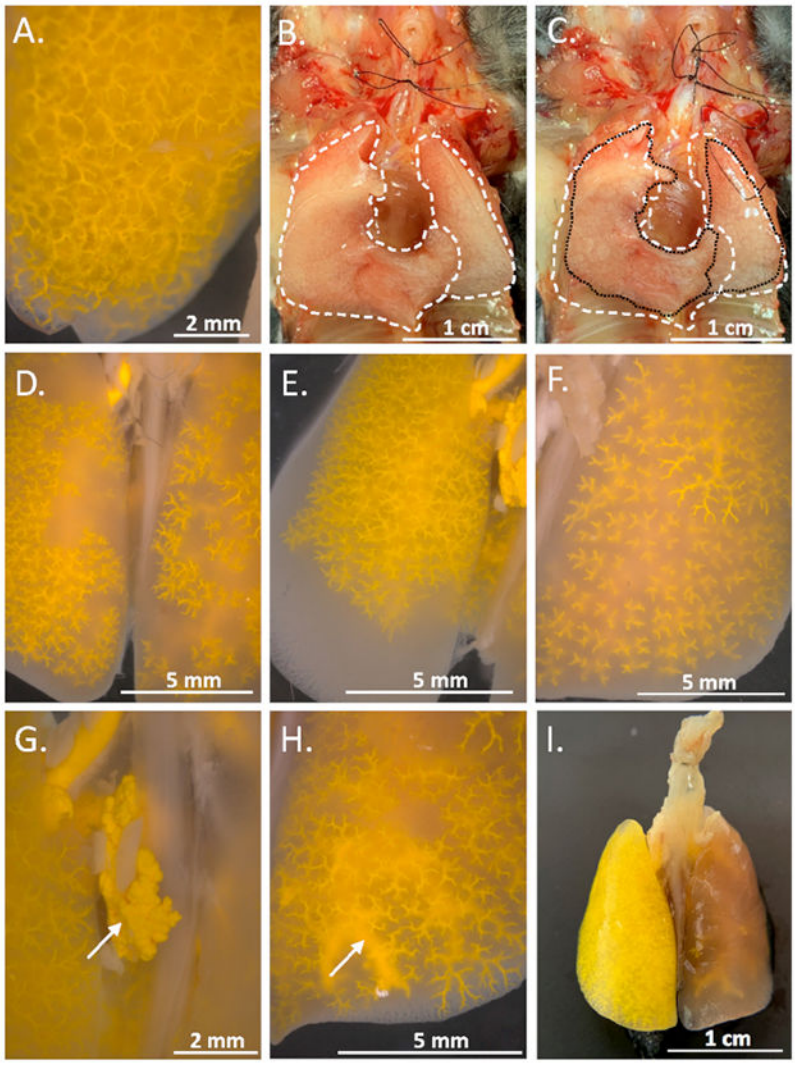

Figure 5: Examples of ideal filling and common errors during polymer compound infusion.
(**A**) When filling endpoint was reached, a robust and fine vascular network was observed. (**B**) Fully inflated formalin perfused lungs are represented by a white dashed line, (**C**) Underinflated/deflated lungs are shown. This was observed due to a compromised pulmonary airway. The original inflated position is represented by a white dashed line and the deflated position is represented by a black dotted line, (**D**) Patchy filling: the vasculature of portions of the lobe remains unfilled while other areas were entirely filled, (**E**) Incomplete filling: the polymer compound failed to penetrate entire sections of lung, (**F**) Underfilling: the polymer compound failed to fill distal vasculature, (**G**) Rupture: the arrow is pointing to the polymer compound extruded from vasculature, (**H**) Venous filling: note the arrow pointing to the arterial segments entirely filled and extending into the venous system. Veins and venules were of significantly larger caliber, (**I**) Catheter wedge: Here the catheter was

shunted into one artery preventing the vasculature of the right lobes from filling completely while the left lobe was overfilled.

Author Manuscript Author Manuscript Author Manuscript Author Manuscript

Author Manuscript Author Manuscript Author Manuscript Author Manuscript

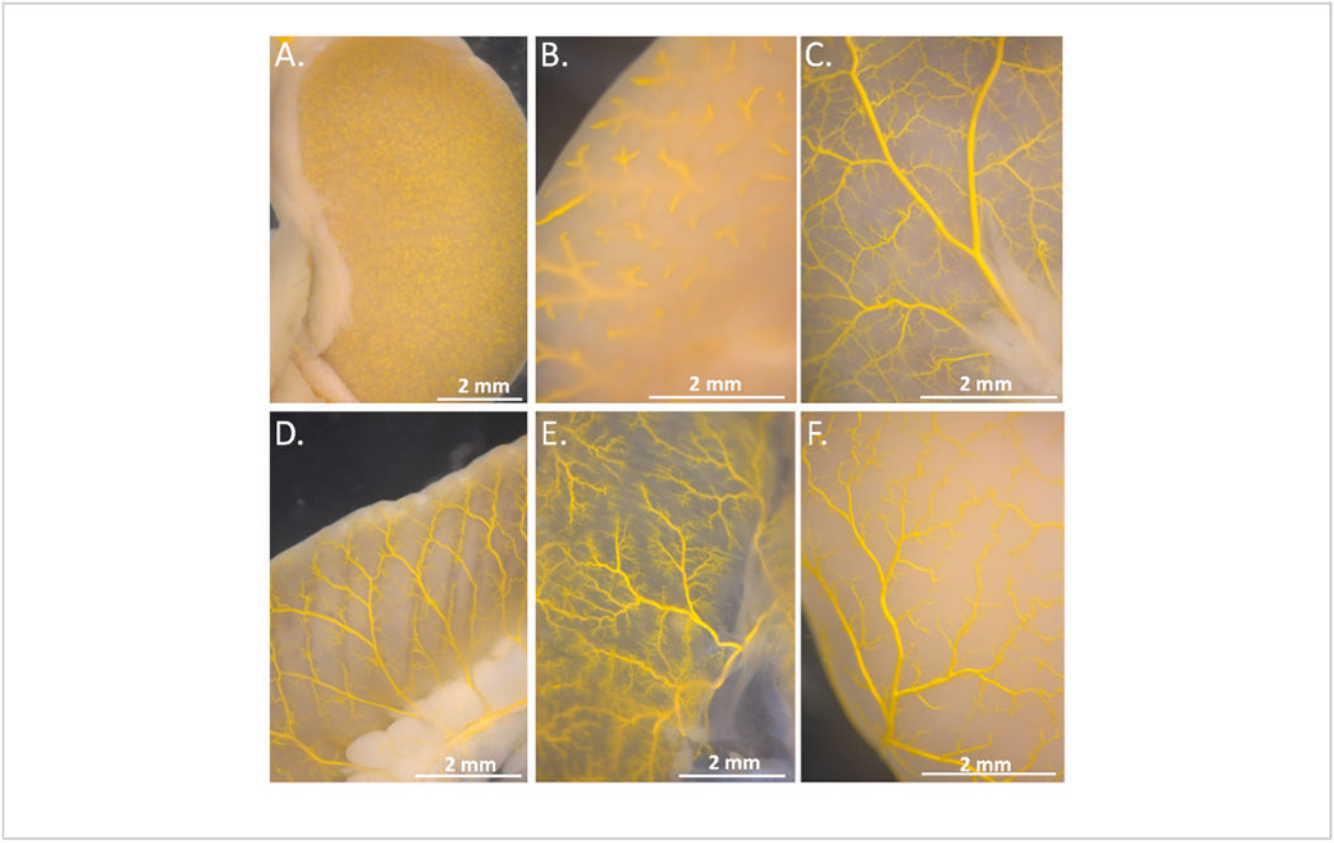

Figure 6. Vascular casting and endpoints in additional organs.

(**A**) Kidney: the punctate appearance of polymer compound in the glomerulus provided the endpoint. (**B**) Liver: note the small vessels visible at the edges of the organ. (**C**) Stomach: small vessels were visible and fully filled. (**D**) Large intestine: Small vessels are easily identifiable and filled. (**E**) Diaphragm: the muscle here is thin and translucent with small filled vessels apparent. (**F**). Brain: small vessels were visible in the cortex.

Author Manuscript Author Manuscript Author Manuscript Author Manuscript

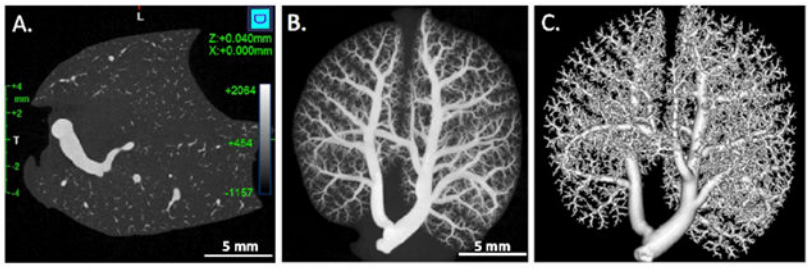

Figure 7. CT images and 3D volume rendering of polymer compound filled lungs.

(**A**) A single grey-scaled reconstructed lung slice, (**B**) This was a maximum intensity projection of a CT scan produced from polymer filled lungs, (**C**) A 3D volume rendering of the vascular arcade was generated using commercially available software (see Table of Materials).

Author Manuscript Author Manuscript Author Manuscript Author Manuscript

Table 1.

Casting alternative vascular beds.

Target Arterial Vascular Bed	Catheter placement	Infusion direction	Infusion rate	Notes
Brain	Thoracic aorta pointing cranially	Retrograde into the carotids	.05ml/min	Cannulate thoracic aorta, flip mouse to the prone position, open scalp, and visually monitor progress of polymer through skull.
Diaphragm	Left Ventrical	Anterograde into internal thoracic, phrenic, and intercostal	.05ml/min	Open a window in the side of the ribcage, leaving the majority of the ribcage and the diaphragm intact. Cannulate left ventrical, clip right atrium, and monitor progress from the caudal side of the diaphragm.
Upper limb musculature	Thoracic aorta pointing cranially	Retrograde into the brachiocephalic and left subclavian	.02ml/min	To optimize limb flow, tie off the carotid arteries and remove limb skin to allow visual monitoring of polymer transit into the limb musculature.
Kidney	Thoracic aorta pointing caudally	Anterograde into renal arteries	.05ml/min	The internal vasculature is filled blindly. To avoid venous transit, stop injecting when polymer is visible in a uniform punctate pattern across kidney.
Portal System	Portal vein	Anterograde into portal system	.02ml/min	Gently fold liver up to expose the portal vein.
Hepatic	Thoracic aorta pointing caudally	Anterograde into the hepatic artery	.05ml/min	Tie off portal vein prior to infusion to avoid venous transit from gut flowing into liver.
Stomach/ Intestine	Thoracic aorta pointing caudally	Anterograde into the celiac, superior mesenteric and/or inferior mesenteric	.05ml/min	Some regions of the gut are supplied by multiple arteries and may fill at different times. To avoid venous transit, tie off arteries not required for areas of interest and visually monitor the progress of the polymer.
Intra-abdominal fat pads	Thoracic aorta pointing caudally	Anterograde but vessel depends on fat pad being studied	.05ml/min	Fat pads are supplied by multiple arteries and may fill at different times. To avoid venous transit, tie off arteries not required for precise area of interest and visually monitor the progress of the polymer.
Lower limb musculature	Infrarenal aorta pointing caudally	Anterograde into the femoral arteries	.02ml/min	Remove limb skin to allow visual monitoring of polymer transit into the limb musculature.

Author Manuscript Author Manuscript Author Manuscript Author Manuscript

Table 2.

µCT Scanning Parameters.

CT settings	
kVp	90
Target Material	Tungsten
Power	8W
Filtration	Cu 0.06 mm + Al 0.5 mm
Projection Number	6424
Detector Size	Flat panel CMOS - 2944 x 2352 pixels
Field of View (FOV)	36 mm
Voxel Size	72 µm
Spatial Resolution	voxel size x 1.5
Acquisition Time	14 min
Reconstruction	FBP and commercial algorithm
Binning	1x1